Neutron scattering studies of the vortex lattice in niobium and ℜ123 superconductors (invited)

N. Rosov, J. W. Lynn,[a] and T. E. Grigereit[a]
Reactor Radiation Division, National Institute of Standards and Technology, Gaithersburg, Maryland 20899

The magnetic flux lattice undergoes a melting transition not only in high-T_c oxide superconductors, but also in conventional superconductors, as recently observed in superconducting niobium films. Small-angle neutron scattering was used to investigate the properties of the magnetic flux lattice in a large, high-quality single crystal of niobium. The small London penetration depth of niobium gives a large magnetic scattering signal, and the use of a high-quality single crystal eliminates other unwanted scattering (from twin boundaries, voids, etc.). The signal-to-noise ratio is therefore improved by several orders of magnitude over the best available measurements of high-T_c oxide superconductors. A sixfold hexagonal pattern of peaks is observed in the mixed state ($H_{c1}<H<H_{c2}$) at all temperatures. These peaks are resolution limited below the irreversibility line; above it, the width in the transverse direction increases with temperature due to the vortex dynamics. Close to H_{c2}, the radial widths of the peaks also broaden. The increase in broadening is a direct observation of a transition to a disordered phase. Nevertheless, the basic hexagonal pattern of peaks is maintained throughout the mixed state, indicating that a correlated flux fluid exists in the reversible regime. Some results on the vortex lattice in superconducting $DyBa_2Cu_3O_7$ are presented and some of the possible exotic states resulting from the coexistence of antiferromagnetic order and superconductivity are described.

I. INTRODUCTION

The melting of the flux lattice in high-temperature oxide superconductors is currently a subject of great fundamental and practical interest. The early discovery of an irreversibility line[1] in the cuprate superconductors suggested that the basic vortex behavior was quite different from previously known superconductors, perhaps due to the much higher critical temperature T_c. Neutron scattering studies of the melting process to probe the exact nature of the melting transition would be most interesting, especially since techniques such as Bitter decoration are restricted to low fields. Unfortunately, the very nature of the high-T_c superconductors makes observing such a melting transition via neutrons extremely difficult. The London penetration depth λ_L in the oxide superconductors is a factor of 4 or 5 larger than for niobium (for which $\lambda_L \approx 350$ Å). As a result, the neutron scattering intensity from the flux lattice, which goes as λ_L^{-4}, is much smaller for the high-T_c materials. An additional technical difficulty is that presently available large single crystals of 123 superconductors have grain boundaries, twin boundaries, and various other defects that give rise to scattering in the same small-angle region as the vortex scattering. This dramatically reduces the signal-to-noise ratio for the vortex scattering, and makes the vortex scattering pattern much more difficult to study.

Irreversibility lines have also been recently observed in niobium, which is an ideal candidate for neutron studies of the vortex lattice, with the combined benefits of large signal and low background due to the availability of large, high-quality single crystals. Pure, defect-free niobium has a Ginzburg–Landau parameter κ of 0.77, just slightly greater than the minimum value $(1/\sqrt{2})$ for type II behavior. In addition, niobium is a material for which κ can be dramatically increased by the influence of defects such as grain boundaries or by the introduction of impurities. Neutron diffraction experiments on the flux line lattice in niobium have been performed over the last thirty years, beginning with a study by Cribier *et al.*[2] that explicitly demonstrated the existence of a triangular vortex lattice, and continuing with much more detailed work by groups at Jülich[3] and Oak Ridge.[4] The subsequent work focused on the interaction of the flux lattice with the crystalline lattice, concentrated mainly on the region of the phase diagram well below the upper critical field $H_{c2}(T)$. The work[5] that we review here extends the measurements to the $H_{c2}(T)$ line.

In the first part of this article we describe the basics of the neutron scattering experiments and the features of the vortex lattice over the (H,T) plane in niobium. We continue with a description of our detailed measurements of the melting of the vortex lattice in niobium and conclude with a description of some recent work on rare-earth 123 superconductors.

[a]Also at the Center for Superconductivity Research, Department of Physics, University of Maryland, College Park, MD.

 0021-8979/94/76(10)/6772/6/$6.00

II. EXPERIMENT

A. Neutron scattering

The bulk of the experimental results described here were obtained on the 30 m small-angle neutron scattering (SANS) spectrometers of the Cold Neutron Research Facility at the National Institute of Standards and Technology. Both spectrometers operate in the same way: A beam of neutrons moderated by a cold source is incident on a neutron velocity selector, which produces a triangular wavelength distribution of neutrons with $\Delta\lambda/\lambda \approx 15\%$. The neutrons pass down a long ($\lesssim$15 m) variable-length flight path with a pinhole collimator at each end, which fixes the incident neutron momentum $\mathbf{k}_i$. After the sample there is another variable-length flight path to a multidetector, which allows the simultaneous collection of data over some range of momentum transfer $\mathbf{Q}=\mathbf{k}_i-\mathbf{k}_f$.

Our sample is a 95 g single crystal of niobium, 9 cm in length, with a diameter of 1.25 cm. The cylinder axis is the [110] crystallographic axis, which was oriented perpendicular to the applied field. The neutron beam illuminated a section of approximately 1 cm diameter near the midpoint of the cylinder. Initial measurements were performed in a flow cryostat with an Al vacuum shroud and 77 K heat shield that was mounted in an electromagnet with holes for the neutron beam drilled through the pole pieces. Later measurements were performed in a horizontal superconducting magnet cryostat specially designed for SANS measurements, with single-crystal sapphire windows along the beam path to reduce unwanted cryostat scattering.

At low temperatures a crystalline vortex lattice is formed, and the scattering pattern of neutrons from the flux lattice directly reveals the reciprocal lattice. Our experimental configuration involved applying the magnetic field nearly along the incoming neutron direction $\mathbf{k}_i$. In this case, the possible momentum transfers for all six 10 reflections are approximately parallel to the plane of the detector, so a pattern such as Fig. 1 will appear on the detector. The simultaneous appearance of all six spots in this case results from some domain structure in the formation of the lattice. If the lattice is formed carefully, it is possible to observe a single diffraction spot as in Fig. 1(bottom).

This pattern [Fig. 1(top)] was collected in two minutes. In comparison, a similarly sized single crystal of $YBa_2Cu_3O_7$ (Ref. 6) requires the subtraction of a zero-field cooled background scan from the applied field scan, each of which takes several hours counting time. The excellent quality of the Nb single crystal—with an almost complete lack of sample-dependent small-angle scattering, incoherent scattering, and absorption—not only allowed the rapid collection of data in the low-temperature regime, but in fact permitted the analysis of the behavior near the H_{c2} phase boundary, where the signal is drastically reduced.

The reciprocal lattice of a triangular lattice with lattice constant a is a self-similar triangular lattice with lattice constant $a^*=4\pi/\sqrt{3}a$. Since the flux quantum $\phi_0=2.068\times10^{-15}$ T m^2 and the area per flux quantum is $\sqrt{3}a^2/2$, we can relate the internal magnetic field B to the lattice parameter by $\phi_0=\sqrt{3}Ba^2/2$. The position in reciprocal

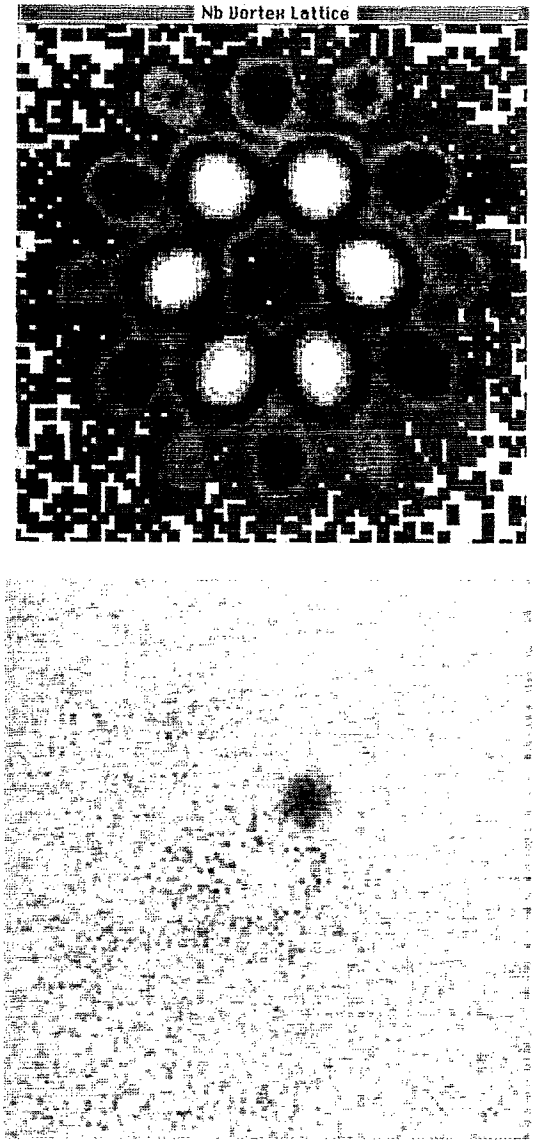

FIG. 1. (Top) Sixfold scattering pattern as observed on the two-dimensional multidetector from single crystal niobium at $T=4.5$ K and $\mu_0H=0.12$ T. The gray-scale image is logarithmically scaled. (Bottom) Pattern of a single diffraction spot obtained at 6.85 K and $\mu_0H=0.12$ T. Here the gray scale is linear.

space of the 10 reflection, which occurs at a momentum transfer $Q_{10}=a^*$, is

$$Q_{10}=2\pi\sqrt{2B/\sqrt{3}\phi_0}. \tag{1}$$

In the $\mathbf{H}\|\mathbf{k}_i$ configuration, there are a number of ways to view the data. One way is a "radial scan," which is performed by summing the scattering at a particular Q around a portion, or all, of the detector [see Fig. 2(a)]. These scans (or sums, in this case) determine the translational correlations between the flux lines in the lattice. Another possibility is a "transverse scan," a sum of the scattering over a small range of Q as a function of angle ϕ around the detector [see Fig. 2(b)], which gives the angular correlations between the flux lines. Finally, we can perform rocking scans [see Fig. 2(c)], where the intensity in a particular region of the detector is

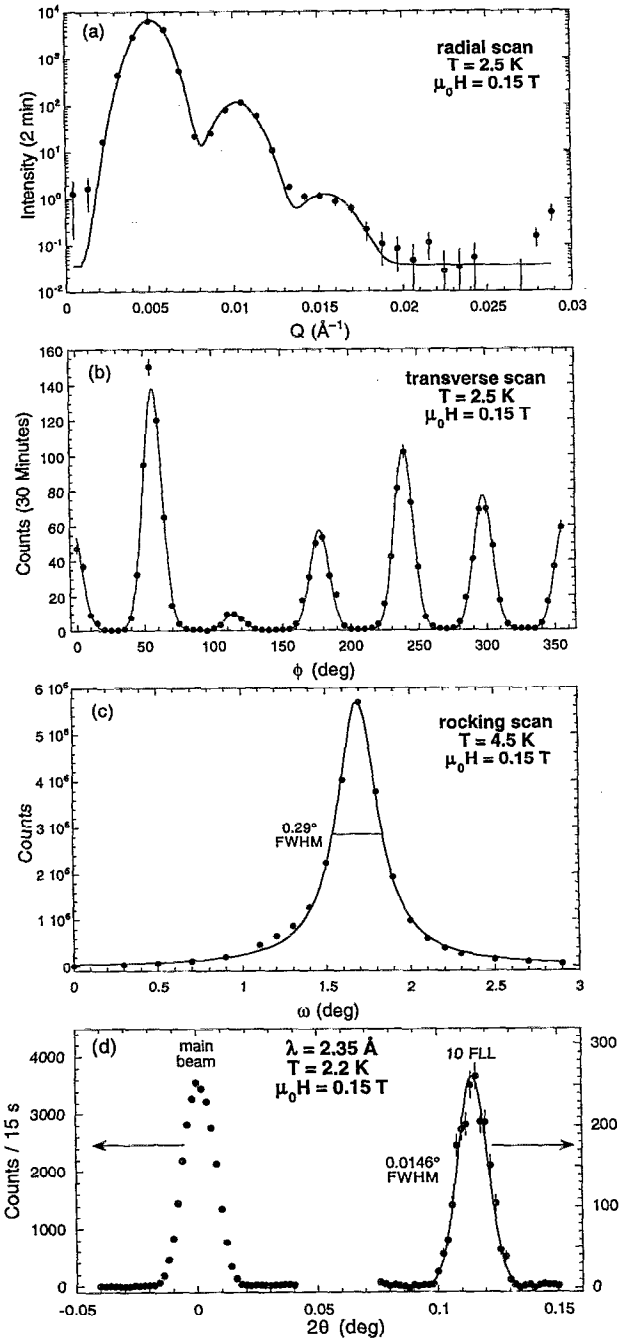

FIG. 2. Various summations of the Fig. 1(top) pattern: (a) Radial and (b) transverse scans at $T=2.5$ K and $\mu_0 H=0.15$ T. (c) Rocking curve of Nb as collected on the SANS spectrometer: total intensity in the peak as a function of magnet angle. (d) Radial scan of 10 peak with improved resolution performed on the BT-7 reflectometer.

recorded as a function of magnet rotation angle ω. In this configuration, the rocking scans primarily determine the straightness of the flux lines.

B. The flux line lattice in Nb

In the Meissner state, the magnetic field in the sample must vanish, i.e., $\mathbf{B}=0$. The magnetization $\mathbf{M}$ of the sample then depends directly on the applied magnetic field $\mathbf{H}_{\rm app}$ to produce the required cancellation. The boundary conditions on the field imply a demagnetizing field, due to the sample magnetization, that opposes the applied field, and so

$$\mathbf{H}=\mathbf{H}_{\rm app}-\eta\mathbf{M}, \tag{2}$$

where η is the demagnetization factor. In the case of an infinite right cylinder with a field applied perpendicularly to the cylinder axis $\eta=1/2$, the H inside the sample is actually $2H_{\rm app}$ in the Meissner state. For the internal field to reach the lower critical field H_{c1}, a field $H_{\rm app}=\frac{1}{2}H_{c1}$ needs to be applied.

For $H_{\rm app}\geq\frac{1}{2}H_{c1}$, flux will penetrate the sample. The competition between the short-range repulsion and long-range attraction of the fluxoids initially causes the formation of domains of flux lines with a density B_0 determined by the strength of the long-range attraction. In this intermediate mixed state (IMS), the sample magnetization is $\mathbf{M}=f\mathbf{B}_0/\mu_0-\mathbf{H}$, where f is the fraction of the sample in the vortex state. As the applied field is $\mathbf{H}_{\rm app}=\mathbf{H}+\eta\mathbf{M}$, in the IMS the relation between the applied field and the internal fields is

$$\mathbf{H}_{\rm app}=(1-\eta)\mathbf{H}+f\eta(\mathbf{B}_0/\mu_0). \tag{3}$$

In our experimental configuration, f increases linearly from 0 at $H_{\rm app}=\frac{1}{2}H_{c1}$ to 1 at $H_{\rm app}=\frac{1}{2}H_{c1}+\frac{1}{2}B_0/\mu_0\equiv H_2$. With further increase of $H_{\rm app}$ above H_2, the flux lattice density increases throughout the sample. Just below H_{c2} the flux lattice achieves its highest density, and ultimately, at $H_{\rm app}=H_{c2}$, the sample magnetization goes to zero and the sample is no longer superconducting.

We thus expect to observe the following behavior as a function of field in a SANS measurement: For $H_{\rm app}<\frac{1}{2}H_{c1}$ the sample is in the Meissner state and there is no scattering. Just above $\frac{1}{2}H_{c1}$ flux penetrates the sample and is confined to regions with constant flux density B_0; elsewhere in the sample, the flux density is zero. At this point, a scattering pattern can be observed, with a lattice spacing corresponding to the flux density B_0,

$$a_0=\sqrt{\frac{2}{\sqrt{3}}\frac{\Phi_0}{B_0}}. \tag{4}$$

This lattice spacing remains constant while the scattering intensity increases linearly with field, until $H_{\rm app}=H_2$, where the flux lattice fills the entire sample. Above H_2, the flux density increases, but the scattering intensity decreases as the fluxoids overlap each other and the contrast is consequently reduced. The sample magnetization is $\mathbf{M}=\mathbf{B}/\mu_0-\mathbf{H}$, so the flux density is then $B=\mu_0[H_{\rm app}-(1-\eta)H]/\eta$. Exactly this behavior has been observed for niobium by Christen *et al.*[4]

We can also make the SANS measurements as a function of temperature in a constant applied field. Since $H=-M+B/\mu_0$, then

$$B=\mu_0(H_{\rm app}+\tfrac{1}{2}M) \tag{5}$$

for our experimental configuration. As the magnetization is negative and approaches zero near the superconducting phase boundary, the flux density increases as the phase boundary is approached, and so the diffraction peaks move out from their low-temperature position. Since the magneti-

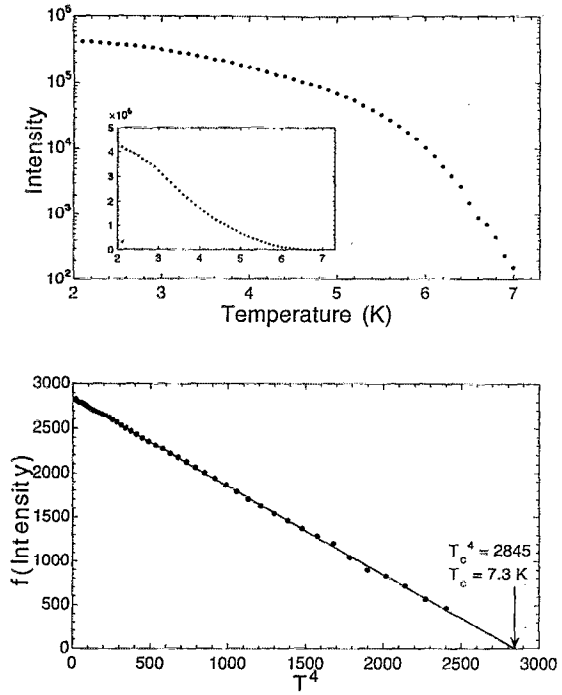

FIG. 3. (a) Intensity of the 10 peak as a function of temperature and (b) linearized plot of $f(I)$ vs T^4, showing the extrapolation to obtain $T_c(H)$.

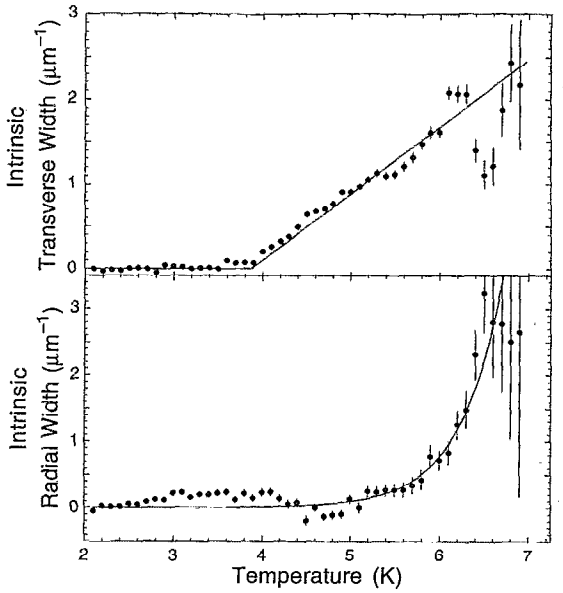

FIG. 4. Intrinsic transverse (top) and radial (bottom) widths as a function of T.

zation goes to zero at H_{c2}, the demagnetization factor does not affect the determination of the upper critical field, and the magnetic scattering will disappear at $H_{\rm app}=H_{c2}$.

III. MELTING OF THE FLUX LATTICE IN NIOBIUM

The observation of irreversibility lines and the implication of melting phenomena occurring in the flux lattice of the high-T_c superconductors prompted a reexamination of "conventional" superconductors to see if similar phenomena were possible in these systems. Drulis *et al.*[7] observed irreversibility effects from flux depinning in vibrating reed measurements on cold-rolled niobium foils. Later work by Schmidt *et al.*[8] demonstrated the existence of a magnetic irreversibility line in sputtered Nb films that followed the expectations for a melting line.

One would naively expect that the melting of the flux line lattice might be manifested by a sudden transition from the low-temperature hexagonal pattern of Fig. 1 to an isotropic ring of scattering on the detector, indicative of an isotropic liquid state. We therefore performed field cooling measurements, starting well above the superconducting transition at constant $H_{\rm app}$, and then slowly (<0.1 K/5 min and even slower near the H_{c2} line) lowered the temperature, collecting scattering patterns at various temperatures. Care was taken to avoid overshooting the new temperature set point on changing the temperature. From our discussion above, we expect the intensity to appear just below $T_c(H)$, as the magnetic contrast appears, and this is in fact what happens [see Fig. 3(a)]. We note that since κ is small for our niobium sample, the two-fluid model does not exactly apply; however, we have used the T^4 behavior of the London model to guide us in linearizing the temperature dependence of the scattering intensity, and so allow the extrapolation of the intensity to zero and the determination of $T_c(H)$ [Fig. 3(b)]. From our temperature scans we were able to determine the H_{c2} phase boundary. In addition, we immediately noticed that (i) the temperature dependence of the scattering was smooth, with no discontinuities; (ii) the scattering intensity was not lost until just below the extrapolated H_{c2} line; and (iii) we always had a sixfold pattern—no ring of scattering ever appeared. Not only did the scattering from the vortices maintain its hexagonal symmetry at all fields and temperatures in the mixed state, but it was locked by the crystalline anisotropy, since we consistently observed the same orientation for the sixfold diffraction pattern over many different experimental configurations.

If, however, we examined the widths of the peaks in the radial and transverse directions as a function of temperature, we found (see Fig. 4) that at some temperature $T_t(H)$ well below $T_c(H)$, an intrinsic width developed in the transverse direction. This width determines the degree of orientational correlations. The radial width remained resolution limited until some higher temperature $T_r(H)$, whereupon it also developed an intrinsic width. We also measured the scattering pattern from the vortex lattice on the NIST BT-7 reflectometer. The spectrometer resolution here is a factor of 3 better for radial scans than the corresponding SANS resolution [see Fig. 2(d)]. We observed the radial width increase above the resolution limit with the reflectometer at the same temperature as we had observed on the SANS, and this therefore lends confidence the intrinsic radial widths develop at higher temperatures than the intrinsic transverse widths.

To further clarify the nature of these two transitions, we performed isothermal field sweeps and found that the peak intensities and widths were reversible above the T_t line and hysteretic below. The restoration of the reversible behavior above T_t leads us to believe that we have observed the onset of a correlated flux fluid state above T_t. This state may not

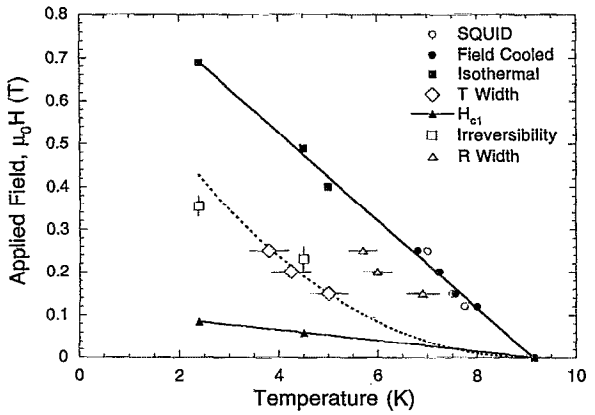

FIG. 5. Phase diagram H vs T for Nb as determined by neutron scattering. The H_{c1} and H_{c2} boundaries are indicated, as are the points where the radial and transverse widths broaden.

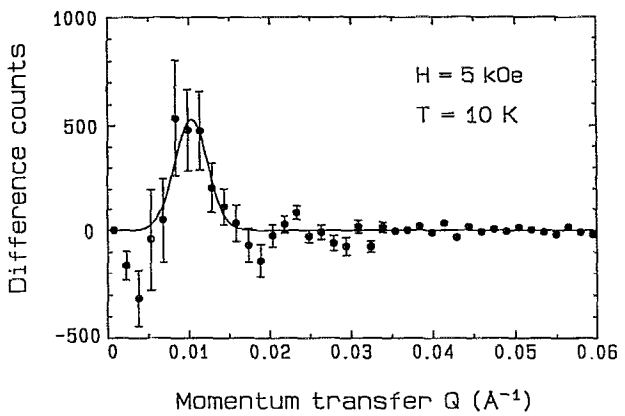

FIG. 6. Radial sum of the difference pattern between field-cooled and zero-field cooled Dy123 at $T=10$ K and $\mu_0 H=0.5$ T. The peak position indicates that the lattice is close to triangular.

be a hexatic phase, since in hexatic systems both the transverse and radial widths appear to be coupled and therefore the intrinsic widths would be expected to develop together.[9]

Figure 5 displays the experimentally determined phase diagram for our niobium crystal. The lower and upper critical fields have been determined via neutrons by the respective onset and loss of scattering from the flux lattice. We can estimate from the two-fluid model that $\kappa \approx \sqrt{H_{c2}/H_{c1}} \approx 2$. This is larger than the value of $\kappa \approx 0.8$ obtained for high purity and defect-free niobium.[4,10] Our sample and those of Drulis *et al.*[7] and Schmidt *et al.*[8] are high purity niobium; however, the various preparation methods created samples with varying defect and grain boundary concentrations, as reflected by the value of κ. Those samples with larger κ have a larger $H_{c2}(T)$: the $\kappa \approx 7$ cold-rolled foil[7] higher than our sample and the $\kappa \approx 10$ sputtered film[8] still larger. The phase diagram also shows $T_r(H)$, $T_t(H)$, and the irreversibility line $T_{\rm irr}(H)$. The irreversibility line and $T_t(H)$, which we identify with a melting curve, are well below that reported for the cold-rolled foils,[7] which is lower again than the melting curve for the sputtered niobium films.[8] This supports the reasonable expectation that $T_{\rm irr}$ depends on the pinning strength and defect density.

The broadening is definitely dynamic in origin, and there are two possibilities for the behavior which we observe. The first possibility is that the onset of broadening in the transverse width indicates a transition to an orientationally disordered phase and that the broadening of the radial width at a higher temperature is associated with the loss of translational order. In this case, the low-temperature phase is crystalline, the transition to an orientationally disordered phase occurs at $T_t(H)$, and a correlated flux fluid exists above $T_r(H)$.

The second possibility is that the transverse broadening is "lattice dynamical" in origin, associated with the same soft shear mode of the vortex lattice that would be involved in melting. This would imply that if much higher instrumental resolution were available, we would see wings of inelastic scattering on the sides of an elastic Bragg peak. The present (best available) resolution would convolve the elastic and inelastic scattering into a single broadened peak. In this case, we would be observing the effect of the inelastic scattering on the linewidth at T_t, and the lattice would not melt until the intrinsic radial width begins to develop.

Given the correlation between the onset of irreversibility in the isothermal scans and the abrupt onset of an intrinsic transverse width in the constant field scans, we believe that the first explanation is the correct one. We cannot entirely rule out the second; however, in either case we observe a correlated flux fluid, due to the non-negligible interactions of the crystal with the vortices. It is interesting to note that broadening in the radial and transverse widths, similar to what we have observed for this two-dimensional system, has also been observed in melting transitions in two-dimensional colloidal suspensions.[11]

IV. THE FLUX LINE LATTICE IN MAGNETIC ℜ123 SUPERCONDUCTORS

The coexistence of antiferromagnetism and superconductivity poses the question: What is the effect of an underlying magnetic order on the vortex lattice? The high-T_c compounds $DyBa_2Cu_3O_7$ and $ErBa_2Cu_3O_7$ are already known to have a very well-defined zero-field ordering of the rare-earth moments at low temperatures ($T_N \approx 1$ K) (Ref. 12) without significant detriment to the superconductivity. We have observed the flux line lattice in a 250 mg single crystal of $DyBa_2Cu_3O_7$, at 10 K in a 5 T applied field (see Fig. 6), well above any temperature where one would expect any effects from the ordering of the rare-earth sublattice. The 10 peak appears at $Q_{10}=0.0105$ Å^{-1}, which is expected for a vortex lattice that is close to triangular, as has been observed by Keimer *et al.*[13] in $YBa_2Cu_3O_7$.

At lower temperatures there are several possible interesting behaviors. Above the onset of long-range order, the enhanced susceptibility of the rare-earth moments would allow a variation of the rare-earth moment alignment that would decorate the vortices. Since the total magnetic flux must be quantized, the addition of the Dy magnetization $M_{\rm Dy}$ will then give a new momentum transfer for scattering from the vortex lattice

$$Q_{M10}=2\pi\sqrt{2\mu_0(H+M_{\rm Dy})/\sqrt{3}\phi_0}. \tag{6}$$

The measured saturated Dy moment is approximately 7 μ_B, which implies that $\mu_0 M_{Dy} \approx 1$ T. In a 0.1 T applied field, we would then expect that the vortex density would increase by roughly a factor of 3 due to the saturated alignment of the Dy moments.

Below T_N, the Dy magnetization will be close to zero at modest applied fields, and so we would return to the original behavior for the flux lattice. However, another possible behavior below T_N could be observed by applying a field strong enough to put the Dy moments through a metamagnetic or spin-flop transition. If the sample has a nonzero demagnetization factor, there would then be coexistence of "paramagnetic" domains that have a net magnetization, with reflections as described by Eq. (6), and "antiferromagnetic" domains where there is no net magnetization, as described by Eq. (1).[14] Another possibility proposed by Buzdin *et al.* is the existence of two-quanta vortices in metamagnetic superconductors, which could occur if the applied field for the metamagnetic or spin-flop transition is near H_{c1}. In this regime, because of the spatial variation of the vortex field, the metamagnetic transition could be localized to a region near the vortex core and substantially affect the structure of the vortex. Work is in progress to experimentally explore these possibilities.

ACKNOWLEDGMENTS

We thank H. Zhang and T. Clinton for assistance at the early stages of this work, J. Z. Liu and R. N. Shelton for the single crystal of $DyBa_2Cu_3O_7$, J. J. Rush for the Nb single crystal, C. Majkrzak for assistance with the BT-7 reflectometer measurements, and S. Krueger and C. Glinka for much assistance in the smooth operation of the SANS spectrometers. Research at Maryland is supported by the NSF, DMR 93-02380. The NG-3 30 m SANS spectrometer at the NIST Cold Neutron Research Facility is supported by the NSF, DMR 91-22444.

[1] K. A. Müller, M. Takashige, and J. G. Bednorz, Phys. Rev. Lett. **58**, 1143 (1987).
[2] D. Cribier, B. Jacrot, L. M. Rao, and B. Farmoux, Phys. Lett. **9**, 106 (1964).
[3] J. Schelten, H. Ullmaier, and W. Schmatz, Phys. Status Solidi B **48**, 619 (1971); J. Schelten, H. Ullmaier, and G. Lippmann, Z. Phys. **253**, 219 (1972); H. W. Weber, J. Schelten, and G. Lippmann, Phys. Status Solidi B **57**, 515 (1973); G. Lippmann, J. Schelten, R. W. Hendricks, and W. Schmatz, Phys. Status Solidi B **58**, 633 (1973); J. Schelten, G. Lippmann, and H. Ullmaier, J. Low Temp. Phys. **14**, 213 (1974).
[4] D. K. Christen, F. Tasset, S. Spooner, and H. A. Mook, Phys. Rev. B **15**, 4506 (1977); D. K. Christen, H. R. Kerchner, S. T. Sekula, and P. Thorel, *ibid.* **21**, 102 (1980).
[5] J. W. Lynn, N. Rosov, T. E. Grigereit, H. Zhang, and T. W. Clinton, Phys. Rev. Lett. **72**, 3413 (1994).
[6] B. Keimer, J. W. Lynn, R. W. Erwin, F. Doğan, W. Y. Shih, and I. A. Aksay (these proceedings).
[7] H. Drulis, Z. G. Xu, J. W. Brill, L. E. De Long, and J.-C. Hou, Phys. Rev. B **44**, 4731 (1991).
[8] M. F. Schmidt, N. E. Israeloff, and A. M. Goldman, Phys. Rev. Lett. **70**, 2162 (1993); Phys. Rev. B **48**, 3404 (1993).
[9] J. D. Brock, R. J. Birgeneau, J. D. Litster, and A. Aharony, Contemp. Phys. **30**, 321 (1989).
[10] H. W. Weber, E. Seidl, C. Laa, E. Schachinger, M. Prohammer, A. Junod, and D. Eckert, Phys. Rev. B **44**, 7585 (1991).
[11] C. A. Murray and D. H. Van Winkle, Phys. Rev. Lett. **58**, 1200 (1987).
[12] See, for example, J. W. Lynn, in *High Temperature Superconductivity*, edited by J. W. Lynn (Springer, New York, 1991).
[13] B. Keimer, F. Doğan, I. A. Aksay, R. W. Erwin, J. W. Lynn, and M. Sarikaya, Science **262**, 83 (1993).
[14] A. I. Buzdin, S. S. Krotov, and D. A. Kuptsov, Solid State Commun. **75**, 229 (1990).